ADVANCED FUNCTIONAL MATERIALS

FULL PAPER

DOI: 10.1002/adfm.200600462

Magnetic-Core/Porous-Shell $CoFe_2O_4/SiO_2$ Composite Nanoparticles as Immobilized Affinity Supports for Clinical Immunoassays**

By *Dianping Tang*, *Ruo Yuan*,* *Yaqin Chai*, and *Haizhen An*

This study demonstrates a novel approach towards the development of advanced protein assay systems based on physically functionalized, magnetic-core/porous-shell $CoFe_2O_4/SiO_2$ composite nanoparticles. The preparation, characterization, and measurement of the relevant properties of the protein assay system is discussed, and the system is used for the detection of cancer antigen 15-3 (CA 15-3, used as a model here) in clinical immunoassays. The protein assay system, based on nanometer-sized magnetic cores and silica shells, shows good adsorption properties for the selective attachment of CA 15-3 antibodies specific to CA 15-3. The core/shell nanostructures exhibit good magnetic properties, which enables their integration into a quartz crystal microbalance (QCM) detection cell with the help of a permanent magnet. Under optimal conditions, the resulting immunoassay system presents a good QCM response for the detection of CA 15-3, and allows the detection of CA 15-3 at concentrations as low as 1.5 U mL^{-1} (U: units). Importantly, the proposed protein assay system can be extended to the detection of other antigens and biological compounds.

1. Introduction

Substantial efforts have been made worldwide to develop and improve clinical immunoassays with the aim of manufacturing portable and affordable diagnostic devices.[1] In spite of the many advances in this field, there is still a paucity of novel approaches for improving the simplicity, selectivity, and sensitivity of clinical immunoassays, in order to respond to the demands and needs of modern medical diagnostics and biomedical research applications.[2] In this regard, the protein-mediated assembly of nanoparticles is a potent tool for the fabrication of new materials;[1,2] this approach combines tunable nanoparticle features (size, surface functionality, and core properties)[3] with the unique physical and chemical properties of proteins and peptides.[4–10] Here, we have synthesized a novel core/shell magnetic nanomaterial ($CoFe_2O_4/SiO_2$) which is able to form a protein–nanoparticle composite by utilizing the stability of the protein. $CoFe_2O_4$ is a well-known hard magnetic material characterized by very high magnetocrystalline anisotropy, high coercivity, and moderate saturation magnetization;[11] these properties make it a promising material for high-density magnetic data storage.[12] Nanometer-sized silica has been extensively investigated and is known to be an ideal protein host due to its high chemical and thermal stability, large surface area, good dispersibility in aqueous solution, and good compatibility with the environment.[13–18]

The presence of cancer antigen 15-3 (CA 15-3) is frequently used as a marker for breast cancer.[19] Elevated CA 15-3 levels in the blood are found in about 30 % of women with localized breast cancer and in about 75 % of women with invasive breast cancer (cancer that has metastasized or spread to other organs).[20] Numerous analytical techniques based on immunological methods are currently being used to assay CA 15-3, including optical biosensing, fluorometry, imaging ellipsometry, radioimmunoassays, chemiluminescence immunoassays, and enzyme-linked immunosorbent assays (ELISAs).[19–21] Unfortunately, these methods either have low sensitivity and are time-consuming, such as immunofluorescence microscopy, or require expensive instrumentation and technical expertise. Therefore, developing an improved simple and rapid methodology for the determination of CA 15-3 is of considerable interest.

The quartz crystal microbalance (QCM) immunoassay technique offers some key advantages, such as high sensitivity, low cost, real-time output, and label- or radiation-free entities, and thus has been the subject of extensive investigation for use in clinical bioassays and for studying biomolecular interactions.[22,23] However, the immobilization of biomolecules is vital to the successful development of QCM assay systems. In the present paper, we have used the physical characteristics of the nanometer-sized magnetic cores and the good biocompatibility of the silica shells to construct a nontoxic biomimetic interface

[*] Prof. R. Yuan, Dr. D. Tang, Prof. Y. Chai, Dr. H. An
College of Chemistry and Chemical Engineering
Southwest University
Chongqing 400715 (P.R. China)
E-mail: yuanruo@swu.edu.cn

[**] R.Y. gratefully acknowledges financial aid from the National Natural Science Foundation of China (20675064), the Excellent Young Teachers from Chinese Ministry of Education (2002-40), and the Science Foundation of Chongqing (CSTC-2004 BB 4149, 2005 BB 4100). Supporting Information is available online from Wiley InterScience or from the author.

ADVANCED FUNCTIONAL MATERIALS

for the immobilization of CA 15-3 antibodies; this approach provides an environment similar to the native system and allows more freedom of orientation for the biomolecules, thus efficiently retaining the bioactivity of the proteins. Another important issue that needs to be resolved is the ability to regenerate the immunosensor. Although the antigen–antibody linkage can be broken under drastic conditions (e.g., alkaline or acid solutions), these conditions may also adversely impact the immobilized immunoreagents and can even cause them to be released from the immunosorbents. To solve this problem, we have fabricated a new homemade QCM detection cell (Scheme 1a). The functionalized magnetic nanoparticles are attracted to the probe surface with the help of a permanent magnet, thus activating the electrical contact between the immobilized antibodies and the base electrode, which thereby causes the sensor circuit to switch on. Positioning the magnet above the detection cell leads to the retraction of the magnetic nanoparticles from the substrate surface, and the detection circuit is thus switched off, thereby achieving the regeneration of the immunosensor. Thus, the regeneration of the transducer is easily carried out by detaching the permanent magnet from the detection device.

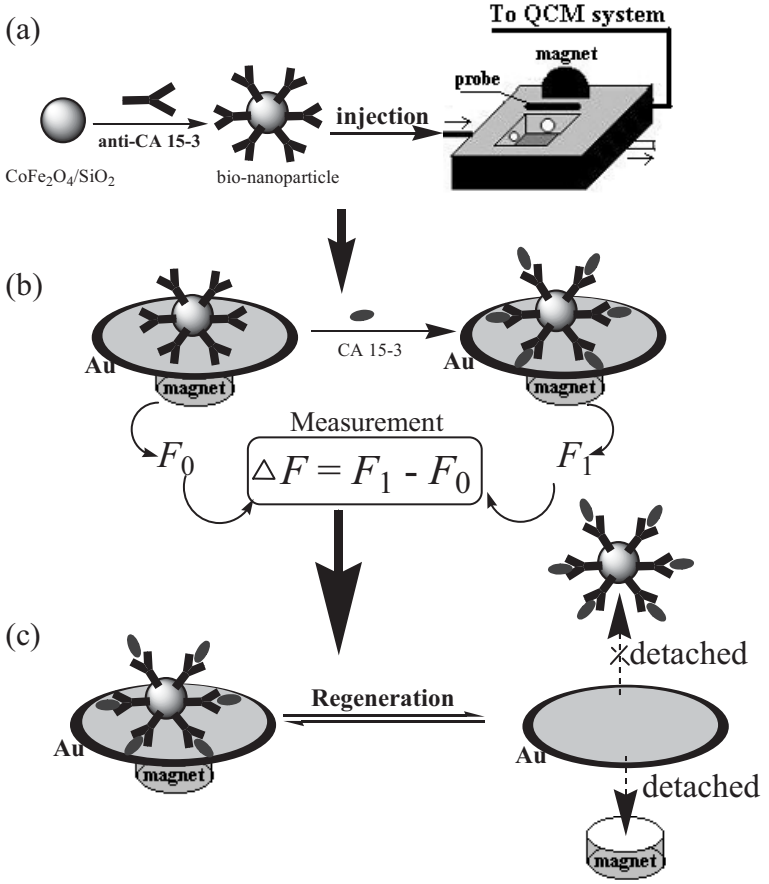

Scheme 1. Schematic illustration of reversible bionanoparticle immobilization and CA 15-3 detection: a) Synthesis of functionalized magnetic bionanoparticles for the QCM assay. b) Biorecognition assay of the QCM system using functionalized magnetic bionanoparticles. c) Regeneration process of the QCM immunoassay system via the detachment and attachment of the external magnet.

In this study, we report a novel protein assay system based on an antigen–antibody reaction that is controlled and switched by means of an external magnet. CA 15-3 antibodies are initially physically attached to magnetic $CoFe_2O_4/SiO_2$ porous nanoparticles; subsequently, the antibody-functionalized composite nanoparticles are attracted to the probe surface with the help of an external magnet. This low-cost and flexible QCM immunoassay system with a flow-injection device provides a simple, sensitive, rapid, and readily regenerable immunoassay for CA 15-3.

2. Results and Discussion

The $CoFe_2O_4$ nanoparticles have been prepared as follows: $Fe(NO_3)_3 \cdot 9\,H_2O$, $Co(NO_3)_3 \cdot 6\,H_2O$, and glycine (Gly) are dissolved in distilled water ($Fe^{3+}/Co^{2+} = 2{:}1$, Gly/nitrate = 4:1, molar ratios). After filtration, the obtained red precursor solutions are concentrated by heating, resulting in the formation of a mixture of amorphous melted salts. Subsequently, a combustion reaction leads to the rapid diffusion of the precursors. Loosely packed black powders ($CoFe_2O_4$ nanoparticles) are obtained after combustion for several seconds. Following the combustion reaction, 0.5 g of the $CoFe_2O_4$ nanoparticles are placed in 10 mL ethanol. This is followed by the sequential addition of 50 mL of deionized water, a certain amount of surfactant, and 30 mL of aqueous ammonia (25 wt %) to the suspension. After stirring the mixture for 40 min, 4.34 g of tetraethoxysilane (TEOS) is added and the suspension is stirred for another 4 h at room temperature. The amount of TEOS is varied to investigate the effect of TEOS on the performance of the $CoFe_2O_4/SiO_2$ composite nanoparticles; 2.14, 3.26, 5.13, and 6.28 g of TEOS have been used to prepare the composite nanoparticles in different experiments. The mixture is then filtered, rinsed with deionized water and ethanol, dried at 150 °C for 2 h, and calcined at 800 °C for 4 h to obtain the $CoFe_2O_4/SiO_2$ composite nanoparticles. The mean sizes of the purified $CoFe_2O_4$ nanoparticles and core/shell $CoFe_2O_4/SiO_2$ nanoparticles, as estimated by transmission electron microscopy (TEM), are 36 and 47 nm, respectively (Fig. 1).

Figure 2 shows an X-ray diffraction (XRD) pattern of the cobalt ferrite sample. The characteristic $CoFe_2O_4$ diffraction peaks gradually grow with increasing cobalt ferrite content, and seem to be the only phase observed by XRD (data not shown). Moreover, the observed peak positions are consistent with the characteristic peaks reported for $CoFe_2O_4$ in the literature.[24] Due to the similar spinel structures of $CoFe_2O_4$ and γ-Fe_2O_3, XRD phase analysis might not be effective at differentiating between the two phases when peak broadening occurs because of the nanocrystalline nature of the sample. In order to confirm the phase purity of the formed $CoFe_2O_4$

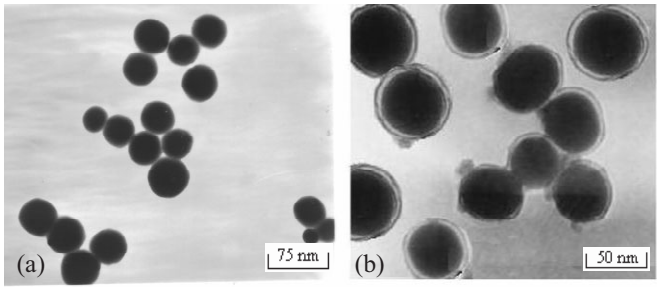

Figure 1. TEM images of a) $CoFe_2O_4$ nanoparticles and b) core/shell $CoFe_2O_4/SiO_2$ nanoparticles.

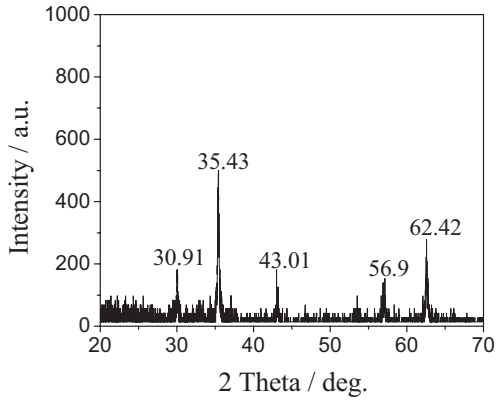

Figure 2. XRD pattern of the $CoFe_2O_4$ sample.

nanoparticles, these samples have also been characterized by Raman spectroscopy (Fig. 3). In the Raman spectra, although most peaks of $CoFe_2O_4$ are close to γ-Fe_2O_3 peaks, γ-Fe_2O_3 exhibits much stronger peaks at 1378 and 1576 cm^{-1} than observed for $CoFe_2O_4$.[25] As shown in Figure 3, very weak peaks are observed in the 800 to 2000 cm^{-1} range for the sample, suggesting that the formation of γ-Fe_2O_3 is very unlikely. Raman peaks observed at 316, 471, and 610 cm^{-1} are characteristic of $CoFe_2O_4$. An important question that still remains is whether a silica shell structure is formed on the nanoparticle surface upon

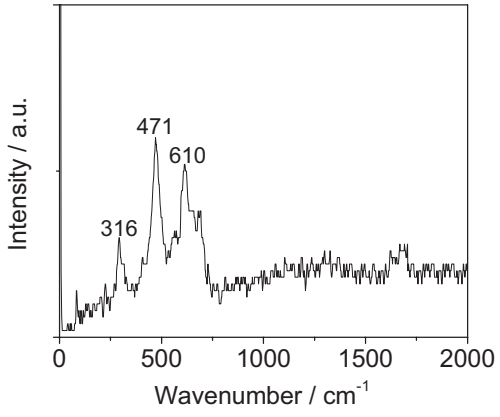

Figure 3. Raman spectrum of the $CoFe_2O_4$ sample.

the addition of TEOS to a mixture containing $CoFe_2O_4$ nanoparticles and aqueous ammonia. We have used inductively coupled plasma atomic emission spectroscopy (ICP-AES) to qualitatively investigate the presence of Co, Fe, and Si. As shown in Figure 4, the prepared composite nanoparticles show characteristic peaks at 238.892, 283.204, and 251.611 nm, confirming the presence of Co, Fe, and Si, respectively.

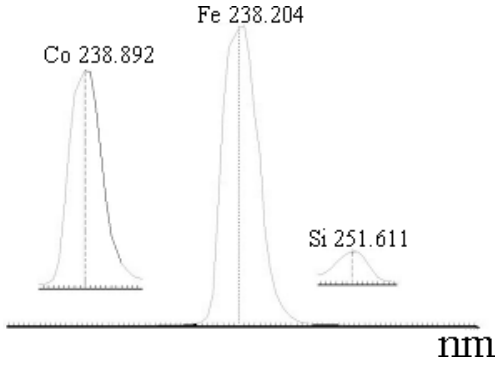

Figure 4. ICP-AES results for a $CoFe_2O_4/SiO_2$ sample.

The interaction between the magnetic $CoFe_2O_4/SiO_2$ porous nanoparticles and CA 15-3 antibodies can be demonstrated using Fourier transform infrared (FTIR) spectroscopy and N_2 adsorption isotherms. As is well known, the shape of the infrared absorption band of amide I groups at 1610–1690 cm^{-1}, corresponding to the C=O stretching vibration of peptide linkages, and of amide II groups around 1500–1600 cm^{-1}, arising from a combination of N–H bending and C–N stretching, can provide detailed information about the secondary structure of proteins.[26–28] The position of the amide I and II bands in the FTIR spectra of proteins is a sensitive indicator of conformational changes in the protein secondary structure,[27] and has been used in this study to investigate immobilized CA 15-3 antibodies. When CA 15-3 antibodies are mixed with a solution of $CoFe_2O_4/SiO_2$ nanoparticles at 4 °C for 14 h under gentle stirring, the amide I and II absorption bands in CA 15-3-antibody-modified immobilized $CoFe_2O_4/SiO_2$ composite nanoparticles are observed at 1640 and 1560 cm^{-1}, respectively (Supporting Information), indicating that the immunoproteins adsorbed on the surfaces of the $CoFe_2O_4/SiO_2$ nanoparticles have retained their native structure.

Proteins can be trapped in the pores of the material by simply immersing the porous $CoFe_2O_4/SiO_2$ composite nanoparticles in the CA 15-3 antibody solution.[29,30] The nitrogen adsorption–desorption curves show a type IV adsorption isotherm and an H1 hysteresis loop for the porous material (Supporting Information).[30] In the 0.7–1.0 Pa range, step-like curves due to capillary condensation in the porous material are observed. The Brunauer–Emmett–Teller (BET) surface area of this material has been determined to be 772.4 $m^2 g^{-1}$. The pore size distribution curve shows a narrow size distribution of the pores with a Barrett–Joyner–Halenda (BJH) average pore diameter of 3.1 nm (Supporting Information).

ADVANCED FUNCTIONAL MATERIALS

With the help of a permanent magnet, the functionalized magnetic composite nanoparticles (denoted hereafter as bionanoparticles) can be physically attached to the probe surface. To further monitor the assembly of bionanoparticles on the gold substrate, and to examine the distribution of the nanoparticles and antibodies on the transducer surface, atomic force microscopy (AFM) measurements have been performed to obtain dynamic images of the two-step process. As shown in Figure 5a, after the attachment of pure magnetic $CoFe_2O_4/SiO_2$ nanoparticles to the gold substrate, the surface roughness ranges from 43 to 57 nm, and some defects are also visible. Figure 5b reveals the broad distribution of bio-nanoparticles after adsorption onto the magnetic nanoparticle surfaces. The surface roughness is greatly reduced, and the surface becomes smooth, which is in accordance with the literature.[31] The origin of the reduced roughness is the filling of the interstitial spaces between nanoparticles by CA 15-3 antibody molecules as a result of their relatively small size when these molecules are assembled onto the composite nanoparticle surfaces. This result proves that antibodies have been immobilized on the gold substrate.

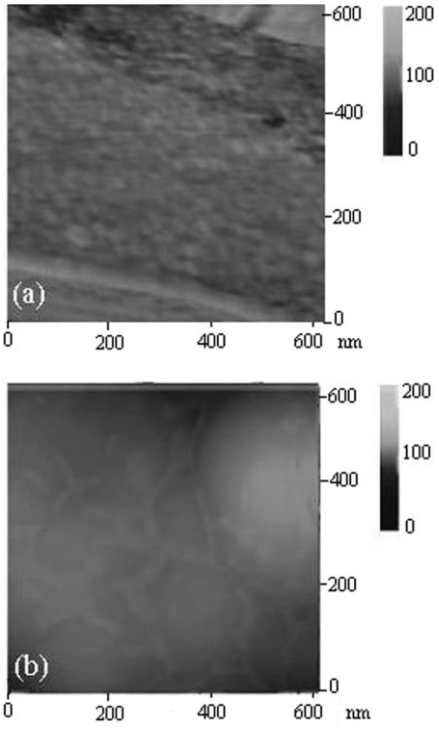

Figure 5. AFM images of surfaces modified by a) pure $CoFe_2O_4/SiO_2$ nanoparticles and b) magnetic bionanoparticles.

The regeneration of immunosensors is of interest to immuno-analysts. In this study, since the bionanoparticles have been immobilized on the probe surface via the exertion of a magnetic force, the magnet plays a critical role in the fabrication of the immunosensor. Scheme 1c shows an illustration of the reversible magnetic-field-induced contacting and retraction of composite magnetic bionanoparticles. Figure 6 shows the regeneration characteristics of the QCM immunosensor; curves b and b′ display the QCM response for the regeneration process. More specifically, real-time QCM measurements have been performed during the two-step process. During the first step, bionanoparticles are assembled on the substrate surface in the presence of a magnetic field (curves a and b, Fig. 6). In the next step, CA 15-3 in the incubation solution reacts with the immobilized CA 15-3 antibodies (curves a′ and b′, Fig. 6). As shown in Figure 6, the magnetic field is detached for the first time after allowing the antigen–antibody reaction to proceed for 140 min. After washing the detection vessel with distilled water, the magnet is attached again, and the same concentration of bionanoparticles (Fig. 6b) and CA 15-3 (Fig. 6b′) is injected sequentially. Comparing curves a and b in Figure 6, the relative standard deviation (RSD) for the same concentration of bionanoparticles is 5.9 %. Similarly, the RSD for 135 U mL^{-1} (U: units) CA 15-3 is 7.9 %. Thus, the QCM immunosensor shows acceptable regeneration performance.

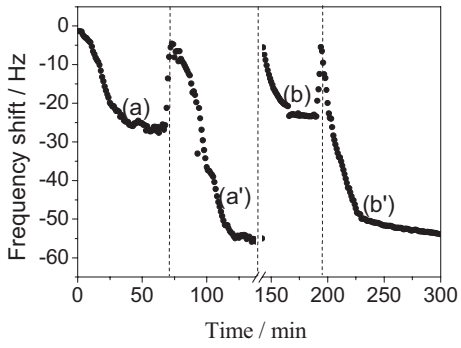

Figure 6. QCM (frequency vs. time) response of the CA 15-3 immunoassay system during two stages of the detection process: first, during the assembly of the magnetic bionanoparticles on the gold substrate (curves a and b); and second, upon reaction between the immobilized CA 15-3 antibodies and CA 15-3 in the incubation solution (curves a′ and b′). The regeneration process is completed by detaching the magnetic field after about 140 min. Curves a and b have been obtained for the same concentration of magnetic bionanoparticles; curves a′ and b′ have been obtained for 135 U mL^{-1} CA 15-3.

To arrive at optimum conditions for CA 15-3 detection using the prepared QCM immunosensor, both the preparation of the magnetic nanoparticles and the sensor fabrication protocol need to be optimized. SiO_2 provides a good surface for subsequent functionalization with CA 15-3 antibody molecules. However, the SiO_2 coating is not sufficiently thick to keep the particles from aggregating. Since ionic capping ligands, which bind to the nanoparticle surfaces, need to be added during nanoparticle synthesis, the electrostatic charge on the ligands leads to electrostatic repulsion, countering the magnetic attraction pulling the particles together. When the SiO_2 coating is too thin, the repulsion between the ligands is less than the attractive magnetic force. As a result, the bionanoparticles tend to aggregate. Thus, 4.34 g of TEOS has been used for the preparation of magnetic core/shell $CoFe_2O_4/SiO_2$ nanoparticles, as shown in Figure 7a. The effect of the strength of the magnetic field at the probe surface on the QCM response of the immunoassay system has also been investigated (Fig. 7b). The high-

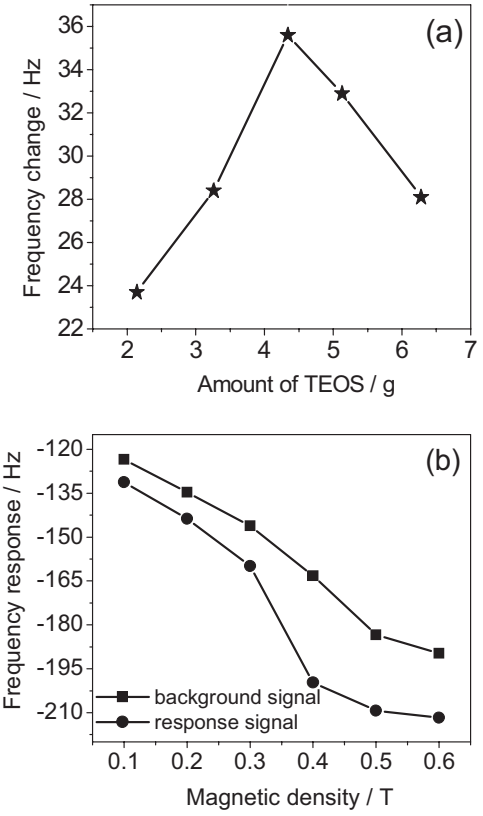

Figure 7. a) The QCM response to 80 U mL^{-1} CA 15-3 using core/shell magnetic $CoFe_2O_4/SiO_2$ nanoparticles prepared by mixing different amounts of TEOS into a solution containing $CoFe_2O_4$ (0.5 g), ethanol (10 mL), deionized water (50 mL), and aqueous ammonia (30 mL, 25 wt%). b) The effect of different magnetic field intensities on the signal-to-background response in the presence (●) and absence (■) of 80 U mL^{-1} CA 15-3.

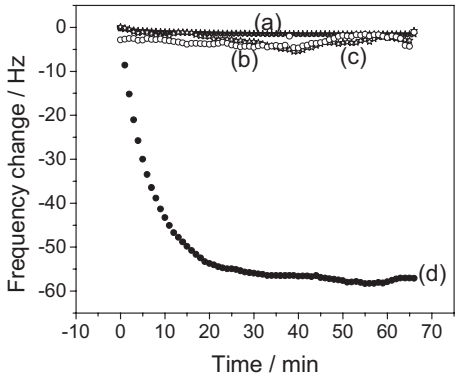

Figure 8. QCM response of the CA 15-3 immunoassay system to different proteins: a) AFP, b) CEA, c) CA 125, and d) CA 15-3 under optimized conditions.

est signal-to-background response is obtained at 0.4 T. A higher signal is observed at magnetic fields larger than 0.4 T; however, the background signal also increases. Therefore, a magnetic field of 0.4 T has been used for QCM measurements of the immunosensor.

Under optimal conditions, the frequency changes increase with increasing CA 15-3 concentration. To investigate the effect of other proteins on the performance of the proposed immunosensors, carcinoembryonic antigen (CEA), carcinoma antigen 125 (CA125), α-1-fetoprotein (AFP) antigen, and the same concentration level of CA 15-3 are separately injected into the measuring cell. Figure 8 displays the typical frequency response curves measured in situ for the different proteins. The control experiments are shown in curves a–c of Figure 8. From Figure 8, it is clear that the frequency change for CA 15-3 is much higher than for the other probes, indicating that there is a significant difference in the response of the target antigen and nonspecific adsorption or crossing recognition. The obtained results indicate that changes in frequency upon nonspecific adsorption are negligible, and that the observed frequency change is caused by the interaction of the antibody with the antigen. Moreover, the frequency response of these probes is also obviously different, presumably due to differences in the degree of interference or crossing-recognition levels among different immunological markers. Additionally, the immunoreaction time is observed to be ca. 30 min. Notably, when normal (negative) serum samples are measured using the QCM immunoassay system in control experiments, the immunosensor shows a negligible frequency response, which is in contrast to results obtained for the CA 15-3-associated samples (data not shown). Such a response level for CA 15-3 can be used as a criterion for judging the immunoreaction data above, wherein a given standard is positively identified or negatively removed.

Figure 9 shows a plot of the change in frequency (ΔF) versus the concentration of CA 15-3. The derived linear regression equation ($R^2 = 0.993$) is given in Equation 1:

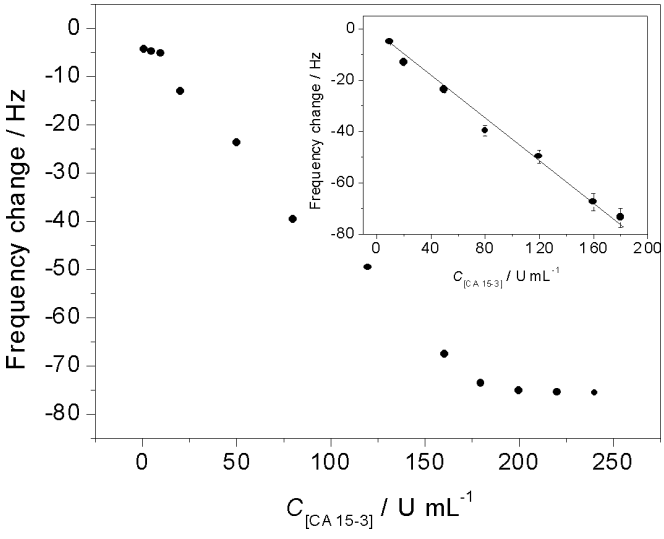

Figure 9. Steady-state calibration plot of the CA 15-3 immunoassay system displaying the frequency shift versus the CA 15-3 concentration under optimized conditions. Each data point represents the average value obtained from three different measurements. The inset shows the linear curve.

ADVANCED FUNCTIONAL MATERIALS

$$\Delta F\,[\mathrm{Hz}] = 4.156 - 0.393 C_{[\mathrm{CA\ 15\text{-}3}]}\,[\mathrm{U\,mL^{-1}}] \quad (1)$$

where $C_{[\mathrm{CA\ 15\text{-}3}]}$ is the concentration of CA 15-3 in the dynamic range between 10 and 180 U mL^{-1} with a detection limit of 1.5 U mL^{-1} (estimated according to International Union of Pure and Applied Chemistry (IUPAC) Recommendation No. 1994).[32] The saturation of the dosage response at higher concentrations of CA 15-3 is mainly due to the limited number of CA 15-3 antibody binding sites. The normal level of CA 15-3 is less than 25 U mL^{-1} in human serum. Thus, the linear relationship is suitable for an "order of magnitude" test of CA 15-3. When the CA 15-3 concentration is more than 180 U mL^{-1}, an appropriate dilution of the sample is necessary for the incubation solution.

The reproducibility of the QCM immunoassay system has been evaluated by intra- and inter-assay coefficients of variation (CVs). The intra-assay CV is the difference between five measurements of one sample using the same batch of magnetic bionanoparticle-modified immunosensors. The inter-assay CV is the difference between five measurements of the same sample using different batches of magnetic bionanoparticle-modified immunosensors. The intra- and inter-assay CVs obtained at a CA 15-3 concentration of 50 U mL^{-1} are 3.7 and 9.8 %, respectively. Occasionally, the prepared magnetic bionanoparticles are difficult to disperse uniformly, which greatly affects the performance of the flow immunoassay system, and results in relatively large variation between different immunosensors. Considering this factor, an inter-assay CV of 9.8 % is acceptable. The low value of the intra-assay CV indicates that the proposed immunosensor can be regenerated and used repeatedly. The acceptable inter-assay CV value verifies the possibility of batch preparation of the magnetic bionanoparticles. When the magnetic bionanoparticles are not in use, they are stored in phosphate buffered saline (PBS) (pH 7.0) at 4 °C. No obvious changes are observed after storing the nanoparticles for four days. Thus, the magnetic core/shell $CoFe_2O_4/SiO_2$ composite nanoparticles are able to efficiently immobilize CA 15-3 antibody molecules.

In order to investigate the possibility of the newly developed technique being used for clinical analysis, ten serum specimens gifted from the Chongqing Institute of Cancer Prevention and Cure have been examined by the developed QCM immunoassay as well as by the reference ELISA method. The measurement method for the serum specimens is as follows: a 30 μL serum sample is diluted with 70 μL PBS (pH 7.0) and injected into the QCM detection cell. The frequency change is recorded versus time. The concentrations of the specimens are evaluated using Equation 1. The results are shown in Table 1. The data shows that there is no significant difference between the results obtained by the two methods, i.e., the data obtained by the QCM assay is consistent with the results obtained using the standard ELISA method. In other words, the developed immunoassay may constitute a promising alternative for determining the concentration of CA 15-3 in human serum in clinical immunoassays.

Table 1. Comparison of CA 15-3 concentrations [U mL^{-1}] in human serum as determined by the as-prepared QCM immunosensor and by the ELISA method. The values shown here are the average values from three different measurements.

Sample number [a]	QCM immunosensor	ELISA	RSD [%]
1	64.5	67.9	2.6
2	38.4	32.4	8.5
3	16.7	18.7	5.6
4	84.9	79.6	3.3
5	125.7	128.4	1.1
6	153.2	147.3	2.0
7	27.3	29.5	3.9
8	12.1	9.4	12.6
9	22.6	25.1	5.2
10	83.7	84.6	0.5

[a] Samples were appropriately diluted using a pH 7.0 PBS solution.

3. Conclusions

Serum CA 15-3 is widely considered to be an especially valuable tumor marker with a threshold value of 25 U mL^{-1} expressed in about 75 % of patients with invasive breast cancer. Here, we report the immobilization of CA 15-3 antibodies on magnetic core/shell $CoFe_2O_4/SiO_2$ composite nanoparticle surfaces; the magnetic nanoparticles are used as matrices for the formation, isolation, and physical separation of biorecognition complexes from complex biological mixtures by means of an external magnet. In other words, the recovery of the functionalized magnetic nanoparticles by means of an external magnet enables their purification by washing and leads to the concentration of the biological recognition pairs. The basic principle of this detection method is the change in frequency before and after the antigen–antibody reaction (Scheme 1b). This low-cost and flexible QCM assay, combined with a flow injection system, provides a simple, sensitive, rapid, and readily regenerable method for the detection of CA 15-3. The magnetic core/shell nanoparticles are able to efficiently immobilize CA 15-3 antibodies. Moreover, the QCM immunoassay system exhibits acceptable precision and reproducibility and provides a one-step method for the rapid determination of CA 15-3 without the need for any separation or washing steps. As compared to conventional ELISA techniques, the method proposed here is reusable, rapid, and easy to automate for high sample throughput. Significantly, this strategy can be readily extended to the preparation of other QCM immunosensors and the detection of other antigens or biomolecules.

4. Experimental

CA 15-3 (0–240 U mL^{-1}) and monoclonal CA 15-3 antibodies (anti-CA 15-3) were purchased from Zhengzhou Biocell Institute (P.R. China). TEOS and bovine serum albumin (BSA, 96–99 %) were purchased from Sigma–Aldrich and used as received. Ammonium hydroxide (30 wt %) and sodium bis(2-ethylhexyl) sulfosuccinate were obtained from Tiantai Fine Chemical (Tianjing, P.R. China). All other reagents

were of analytical grade unless specified and were used without further purification. Deionized and distilled water was used throughout the study. Clinical serum samples were provided by the Chongqing Institute of Cancer Prevention and Cure, P.R. China.

The $CoFe_2O_4$ nanoparticles were characterized by powder XRD (Dmax-2000, Puxi Quanyong, Beijing, P.R. China; with Cu Kα radiation) and Raman spectroscopy (RFS 100/s micro-Raman system, Bruker, Germany). The Raman spectrometer was operated in back-scattering geometry with a helium–neon laser at 1064 nm as the excitation source. The presence of Co, Fe, and Si was confirmed by ICP-AES (Puxi Quanyong, Beijing, P.R. China). FTIR characterization of $CoFe_2O_4/SiO_2$ and $CoFe_2O_4/SiO_2$ with immobilized CA 15-3 antibodies was performed using a Spectrum GX FTIR spectroscopy system (Perkin–Elmer, USA). AFM measurements were conducted using a Digital Instruments (Veeco Metrology Group, USA) microscope. The nanoparticle sizes were confirmed by TEM (H600, Hitachi, Japan). The QCM measurements were performed on 10 MHz QCM devices (Picobalance, Italy). Nitrogen adsorption isotherms were obtained using an ASAP 2000 instrument (Micromeritics, Norcross, GA, USA). Before adsorption measurements, the samples were degassed for 2 h at 150 °C.

The prepared QCM probe was first mounted on one side of the detection vessel containing an assay buffer solution (PBS, pH 7.0, 0.9 % sodium chloride). Each of the samples to be analyzed was then introduced into the detection vessel after stabilization of the resonance frequency (shift less than 1 Hz min^{-1}). To avoid possible errors resulting from the sample addition process and to correct for the response induced by nonspecific adsorption, the frequency changes were recorded as the immunoreaction proceeded from 30 s after the addition of the samples until equilibrium was reached at ca. 30 min. Control tests with normal (negative) samples and evaluation of the clinical specimens was also performed accordingly. The frequency change in all experiments is reported as the average response observed for the immunoreaction over three different measurements along with the corresponding SDs ($\Delta F \pm$ SD), unless otherwise indicated. After each immunoassay run, the contaminated QCM crystals were regenerated by detachment of the magnetic field and washed with doubly distilled water four times before carrying out the next measurement.

In this study, the frequency difference (ΔF_x) was related to the mass accumulation (ΔM) on the quartz crystal electrode surface according to the Sauerbrey equation

$$\Delta F_x = -2.3 \times 10^{-6} F^2 \Delta M / A \quad (2)$$

where ΔF_x is the change in the resonance frequency [Hz], F is the basic resonant frequency of the crystal [MHz], ΔM is the mass accumulation on the crystal surface [g], and A is the deposited electrode area [cm^2]. The frequency shift, ΔF [Hz], is defined as the absolute value of the frequency difference ΔF_x.

Received: May 28, 2006
Revised: August 7, 2006
Published online: February 1, 2007

[1] C. M. Niemeyer, *Angew. Chem. Int. Ed.* **2001**, *40*, 4128.
[2] M. Sarikaya, C. Tamerler, A. K. Y. Jen, K. Schulten, F. Baneyx, *Nat. Mater.* **2003**, *2*, 577.
[3] M. J. Hostetler, J. E. Wingate, C. J. Zhong, J. E. Harris, R. W. Vachet, M. R. Clark, J. D. Londono, S. J. Green, J. J. Stokes, G. D. Wignall, G. L. Glish, M. D. Porter, N. D. Evans, R. W. Murray, *Langmuir* **1998**, *14*, 17.
[4] P. Ringler, G. E. Schulz, *Science* **2003**, *302*, 106.
[5] A. Aggeli, M. Bell, N. Boden, J. N. Keen, P. E. Knowles, T. C. B. McLeish, M. Pitkeathly, S. E. Radford, *Nature* **1997**, *386*, 259.
[6] W. Shenton, S. A. Davis, S. Mann, *Adv. Mater.* **1999**, *11*, 49.
[7] S. Connolly, D. Fitzmaurice, *Adv. Mater.* **1999**, *11*, 1202.
[8] J. Yang, M. Mayer, J. K. Kriebel, P. Garstecki, G. M. Whitesides, *Angew. Chem. Int. Ed.* **2004**, *43*, 1555.
[9] M. R. Robinson, S. Wang, A. J. Heeger, G. C. Bazan, *Adv. Funct. Mater.* **2001**, *11*, 413.
[10] W. Shenton, D. Pum, U. B. Sleytr, S. Mann, *Nature* **1997**, *389*, 585.
[11] X. H. Huang, Z. H. Chen, *Scr. Mater.* **2006**, *54*, 169.
[12] R. A. Sufi, K. Peter, *Macromolecules* **2002**, *35*, 3338.
[13] H. Takahashi, B. Li, T. Sasaki, C. Miyazaki, T. Kajino, *Chem. Mater.* **2000**, *12*, 3301.
[14] D. T. Mitchell, S. B. Lee, L. Trofin, C. R. Martin, *J. Am. Chem. Soc.* **2002**, *124*, 11 864.
[15] Y. J. Han, G. D. Stucky, A. Butler, *J. Am. Chem. Soc.* **1999**, *121*, 9897.
[16] U. Kleitz, F. Wilczok, F. Marlow, *Phys. Chem. Chem. Phys.* **2001**, *3*, 3486.
[17] M. C. L. Maste, W. Norde, A. J. W. G. Visser, *J. Colloid Interface Sci.* **1997**, *196*, 224.
[18] J. Buijs, C. Costa Vera, E. Ayala, E. Steensma, P. Hakansson, S. Oscarsson, *Anal. Chem.* **1999**, *71*, 3219.
[19] H. G. Zhang, C. Qi, Z. H. Wang, G. Jin, R. J. Xiu, *Clin. Chem.* **2005**, *51*, 1038.
[20] J. Kurebayashi, Y. Yamamoto, K. Tanaka, N. Kohno, M. Kurosumi, T. Moriya, R. Nishimura, Y. Ogawa, T. Taguchi, *Breast Cancer* **2003**, *10*, 38.
[21] R. Einarsson, V. Barak, *J. Clin. Ligand Assay* **1999**, *22*, 348.
[22] C. Larsson, M. Rodahl, F. Hook, *Anal. Chem.* **2003**, *75*, 5080.
[23] H. Muramatsu, K. Kajiwara, E. Tamiya, I. Karube, *Anal. Chim. Acta* **1986**, *188*, 257.
[24] International Centre for Diffraction Data (ICCD), Powder Diffraction Database, Pattern 22-1086, **1994**.
[25] M. H. Sousa, F. A. Tourinho, J. C. Rubim, *J. Raman Spectrosc.* **2000**, *31*, 185.
[26] A. Dong, P. Huang, W. S. Caughey, *Biochemistry* **1992**, *31*, 182.
[27] A. Gole, G. Thakar, M. Sastry, *Colloids Surf. B* **2003**, *28*, 209.
[28] J. F. Robolt, F. C. Burns, N. E. Schlotter, J. Swalen, *Chem. Phys.* **1983**, *78*, 946.
[29] J. F. Diaz, K. J. Balkus Jr., *Mol. Catal. B: Enzymatic* **1996**, *2*, 115.
[30] H. Takahashi, B. Li, T. Sasaki, C. Miyazaki, T. Kajino, S. Inagaki, *Microporous Mesoporous Mater.* **2001**, *45*, 755.
[31] J. B. Jia, B. Q. Wang, A. G. Wu, G. J. Cheng, Z. Li, S. J. Dong, *Anal. Chem.* **2002**, *74*, 2217.
[32] R. P. Buck, E. Lindner, *Pure Appl. Chem.* **1994**, *66*, 2527.